Pulsed Eddy Current Sensing for Condition Assessment of Reinforced Concrete

Nalika Ulapane
Electrical and Electronic Engineering
The University of Melbourne
Parkville VIC 3010, Australia
nalika.ulapane@unimelb.edu.au

Sathira Wickramanayake
Centre for Autonomous Systems
University of Technology Sydney
Ultimo NSW 2007, Australia
sathira.wickramanayake@uts.edu.au

Sarath Kodagoda
Centre for Autonomous Systems
University of Technology Sydney
Ultimo NSW 2007, Australia
sarath.kodagoda@uts.edu.au

***Abstract*—Reinforced concrete (i.e., concrete wall–like structures having steel reinforcement rods embedded within) are commonly available as civil infrastructures. Such concrete structures, especially the walls of sewers, are vulnerable to bacteria and gas induced acid attacks which contribute to deterioration of the concrete and subsequent concrete wall loss. Therefore, quantification of concrete wall loss becomes important in determining the health and structural integrity of concrete walls. An effective strategy that can be formulated to quantify concrete wall loss is, locating a reinforcement rod and determining the thickness of concrete overlaying the rod via Non–destructive Testing and Evaluation (NDT & E). Pulsed Eddy Current (PEC) sensing is commonly used for NDT & E of metallic structures, including ferromagnetic materials. Since steel reinforcement rods that are commonly embedded in concrete also are ferromagnetic, this paper contributes by presenting experimental results, which suggest the usability of PEC sensing for reinforced concrete assessment, via executing the aforementioned strategy.**

***Index Terms*—concrete, NDT, NDE, pulsed eddy current, sensor, sewer**

I. Introduction

Pulsed Eddy Current (PEC) sensing, a versatile technique among the Eddy Current (EC) Non–destructive Evaluation (NDE) techniques, has many applications in detection and quantification of defects in metals and metallic structures [1]. The detector coil–based PEC sensor architecture over the years has proven itself to be an effective condition assessment tool for ferromagnetic materials [2, 3, 4, 5]. Motivated by its usefulness, detector coil–based PEC sensors in recent years have been exploited quite effectively for condition assessment of ferromagnetic pipes in the water industry [6, 7, 8, 9, 10, 11].

Alongside condition assessment of water pipes, interest towards condition assessment of waste water pipes, or sewers, also has increased in recent years [12, 13, 14, 15, 16, 17, 18]. Sewer walls are typically made of concrete and a portion of sewer walls carry steel (having ferromagnetic properties) reinforcement rods embedded within. It is common for sewer walls to undergo bacteria and gas induced acid attacks which deteriorate the concrete and cause wall loss leading to weakened structural integrity. Therefore, quantification of concrete wall loss is of interest to sewer infrastructure management. Motivated by this interest, the main contribution of this paper comes in the form of a presentation of experimental results which suggest usability of PEC sensing for condition assessment of reinforced concrete.

Covermeters are typically used for reinforcement rod locating and sizing [19, 20], and are commercially available. As per the authors' experience though, the common availability of covermeters is in the form of manually operated hand–held devices, and not so much as tools that can be automated and interfaced with robotic platforms. On the other hand, authors are fairly experienced in automating and integrating PEC sensors with robotic platforms [21, 22]. Provided some unique hazards such as confined spaces and infectious substances associated with sewers, an increasing demand for robotic means for sewer condition assessment exists. Therefore, PEC sensing may have an edge over covermeters as a result of its established capability for interfacing with robotic platforms, at least when it comes to tasks similar to sewer concrete assessment.

The paper is structured as follows: Section II presents the operating principles of PEC sensing; section III describes the strategies adopted in this paper to enable condition assessment of reinforced concrete; section IV describes conducted experiments and presents their results, and section V concludes the paper while discussing implications of results.

II. Principle of PEC Sensing

Since steel reinforcement rods are ferromagnetic, the detector coil–based PEC sensor architecture is used for the work of this paper. This architecture has been identified in literature [2, 3, 11] to have superior sensitivity to ferromagnetic material volume. The detector coil–based architecture typically comprises two concentrically wound, air cored, conductive circular coils [2, 3, 11]. Rectangular shaped coils too have rarely been used [8], and the signals for this work were captured using oval shaped coils. It is not the intention of the authors to propose an optimal PEC sensor for reinforced concrete assessment in this paper, readers should decide the shape and size of sensors suitable for their application. However, non–circular (i.e., rectangular or oval) sensors are required for the work of this paper. This is the case since circular sensors do not provide information about the orientation of an embedded reinforcement rod, due to circular symmetry of sensors. A PEC sensor design example is available in [23].

Out of the two coils available in the detector coil–based architecture, one coil behaves as an exciter coil while the other behaves as a detector coil which captures the signal. The exciter coil is energized with a voltage pulse which fundamentally takes the shape of a Heaviside step function. The pulsed excitation causes a rapid change in the surrounding magnetic field, which induces time varying eddy currents in any surrounding conductive material (i.e., the reinforcement rod for the work of this paper). The induced time varying eddy currents result in a secondary time varying magnetic field, and the resultant effect of the two magnetic fields induces a time varying voltage (i.e., the PEC signal) in the detector coil which we denote as $V(t)$. $V(t)$ takes the shape of an exponential decay and the typical shape of a signal can be seen in [10, 11]. Previous work [2] has proposed the model in (1) to characterize detector coil–based PEC signals where b_i and c_i are parameters depending on the excitation voltage, sensor characteristics, and electrical and magnetic properties of any surrounding conductive materials.

$$V(t) = \sum_{i=1}^{\infty} b_i \exp\left(-c_i t\right) \tag{1}$$

For the purpose of locating reinforcement rods, and determining the thickness of overlaying concrete, we define the PEC signal feature V_α in (2), where t_0 is a time instance such that $t_0 > 0$. The choice for the value of t_0 is purely dependent on the characteristics of the available sensor and the signals it produces.

$$V_\alpha = \ln[V(t)]|_{t=t_0} \tag{2}$$

A value for t_0 should be chosen through observation, and a strategy for selection is presented in subsection III-B.

III. Strategy for Locating Reinforcement Rods

A. Strategy for selecting PEC sensor shape and size.

Firstly, the size of the expected reinforcement rod should be decided. On occasions, covermeters have been used to estimate the size of reinforcement rods when the size is unknown [20]. For the work of this paper though, authors endeavour to estimate the thickness of concrete overlaying a reinforcement rod (of known size) to determine the degree of concrete wall loss. At a stage where practical application matters, authors do not expect wall deterioration to have reached the reinforcement rods. Therefore, sizing of reinforcement rods is considered out of the scope of the work of this paper. When considering applications such as sewer condition assessment, infrastructure managers usually have archived records which carry specifications such as reinforcement rod sizes. Therefore, the work of this paper relies on the prior knowledge of the size (diameter) of the reinforcement rods. Steel reinforcement rods of 12 mm diameter were used for experiments.

Secondly, the maximum expected thickness of overlaying concrete should be decided upon. Once again, such details become available where technical details and specifications have been archived by infrastructure managers. For the work of this paper, authors have chosen a maximum thickness of 50 mm. According to the targeted application, reinforcement rods may be embedded at different depths, and on occasions, specifications may not be available with infrastructure managers. Therefore in consideration to field applications, it makes sense to be conservative and expect reinforcement rods embedded at larger depths.

On deciding some expected ranges for reinforcement rod sizes and thickness of overlaying concrete, one can use a numerical simulation approach such as Finite Element Analysis (FEA) to perform basic evaluations and determine sensor shapes and sizes adequate for a target application. An example to how FEA has been used in relation to PEC sensing is available in [5]. Alternatively, suitable sizes and shapes can be determined through a few trial and error experiments. Since aligning the PEC sensor to a reinforcement rod becomes advantageous, authors remind the emphasis on designing non–circular sensors.

B. Strategy for selecting a value for t_0.

Two reinforcement rod samples (these samples can be considered as calibration samples) can be placed perpendicular to each other, centred on a grid map as shown at the left of Fig. 1. Since the rod diameter selected for this paper was 12 mm, authors set a grid square size to be 30 mm $\times$ 30 mm (i.e., length of a grid square side = 2.5 $\times$ reinforcement rod diameter). Then, the long side of the non–circular PEC sensor must be aligned to one reinforcement rod, and placed above the rods, at a height equal to the maximum expected overlaying concrete thickness (50 mm for this paper as mentioned in subsection III-A). The grid map should then be covered by the PEC sensor at that height without changing sensor alignment, while recording a signal per grid square. Logarithmic signal instances should then be plotted and visualized in the form of $V_\alpha^{x_i,y_j} = \ln[V(t)]|_{t=t_0}^{x_i,y_j}$, where x_i, y_j are the coordinates of the (i, j) grid location, and t_0 is any time instance such that $0 < t_0 < T$ where T is the PEC signal duration of the available sensor. On observation, it will be possible to identify ranges for t_0 where V_α shows adequate sensitivity to when and when not being on top of reinforcement rods. This sensitivity of V_α is what enables locating reinforcement rods embedded in concrete. For the work of this paper, authors found $t_0 = 5$ ms to be a reasonable value which provides adequate sensitivity to V_α for the target application. Shown at the right of Fig. 1 is a colour–coded V_α plot (yellow indicates high V_α value and blue indicates low V_α value) demonstrating sensitivity to reinforcement rods at the value $t_0 = 5$ ms for the particular PEC sensor used for the work of this paper.

To validate sensitivity at a selected t_0 value, it is recommended to keep the sensor orientation and distance above reinforcement rods as before, and rotate the reinforcement rods to be at an angle to the PEC sensor as shown at the left of Fig. 2, and repeat the experiment to plot $V_\alpha^{x_i,y_j}$ values at the same grid locations. Resulting of a $V_\alpha^{x_i,y_j}$ map having contrast as shown at the right of Fig. 2 indicates the choice of t_0 is adequate for the target application, and can show sensitivity despite reinforcement rods not being aligned with the sensor.

C. Strategy for locating a reinforcement rod.

Shown in Fig. 3 is the strategy for locating a reinforcement rod. Starting at an arbitrary location, the sensor should be translated until it locates a point where a highest V_α value results. As per the observations in subsection III-B, a highest V_α value results when the sensor is on top of a reinforcement rod. This strategy hence locates reinforcement rods.

D. Strategy for aligning the sensor to a located reinforcement rod.

Shown in Fig. 4 is the strategy for aligning the sensor to a located reinforcement rod. Since a PEC sensor selected for this application will be non–circular, it was observed from experimental results in section IV that a highest V_α value results when the longer side of the sensor is aligned with the reinforcement rod while the sensor being on top of the rod. Therefore, after locating the rod through the strategy presented in subsection III-C, by rotating the sensor as in Fig. 4 and searching for a maximum V_α enables aligning the sensor to a rod.

E. Strategy for quantifying overlaying concrete thickness.

Quantification of thickness of overlaying concrete should happen after locating a rod and aligning the sensor. To enable thickness quantification, the system should be calibrated by obtaining a function between distance of the sensor above an aligned rod, and V_α. Results presented in section IV indicate that V_α is also sensitive to distance of the sensor above an aligned rod, which confirms that if calibrated, thickness quantification of overlaying concrete, or simply finding the distance to an aligned reinforcement rod is indeed possible.

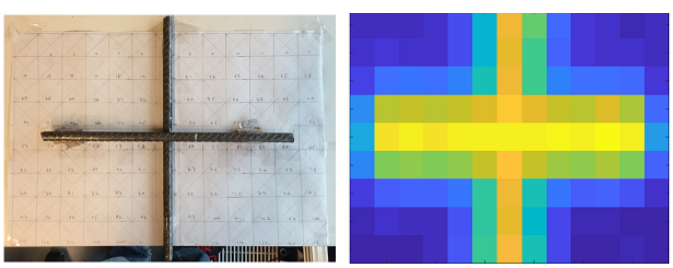

Fig. 1. Setup for determining t_0.

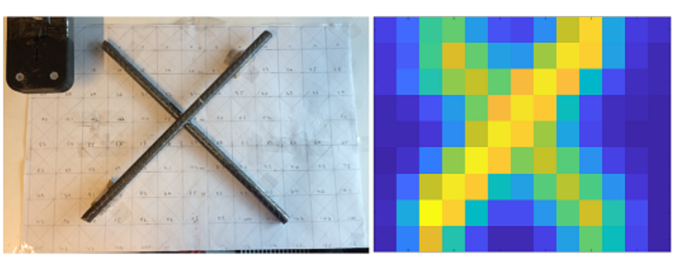

Fig. 2. Setup for validating sensitivity of V_α at $t_0 = 5$ ms.

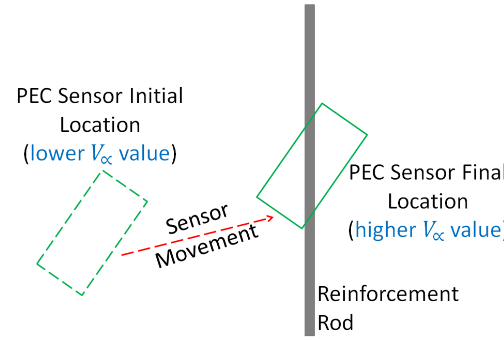

Fig. 3. Strategy for locating a reinforcement rod.

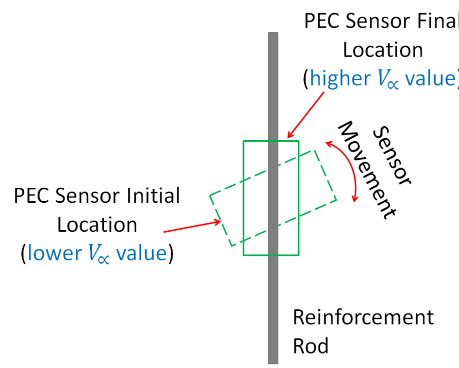

Fig. 4. Strategy for aligning the sensor to a located reinforcement rod.

IV. Experiments and Results

A. Experiment 1: Locating a reinforcement rod.

Experiment 1 was conducted to verify the strategy in Fig. 3 for locating a reinforcement rod by observing variations of V_α. The experimental set–up used is illustrated in Fig. 5. A sample reinforcement rod was placed at different angles from 0^0 to 90^0 with respect to the long side of the PEC sensor, and for each angle, the sensor was translated a horizontal distance of 36 cm as shown in Fig. 5, while the depth to the rod from the sensor was maintained constant at 20 mm. Results observed (i.e., variation of V_α) from this experiment are plotted in Fig. 6. As per the results, it becomes clear that a maximum V_α can be observed when the sensor is right above the rod (i.e., horizontal sensor location = 0 mm as per Fig. 5), except when the angle is 90^0. The 90^0 case becomes slightly complicated. What is indicated by the observations in Fig. 6 is that it is possible to locate a reinforcement rod by means of V_α when the angle is not 90^0. If by chance the 90^0 case is encountered in an application scenario, the difficulty can be countered by translating the sensor in various directions starting from random locations and sensor angles.

B. Experiment 2: Aligning the sensor to a located reinforcement rod.

Once a reinforcement rod is located and the sensor is placed above the rod, it is necessary to align the long side of the

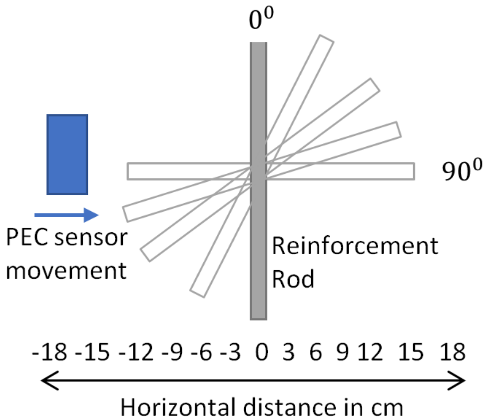

Fig. 5. Experimental set–up for locating reinforcement rod.

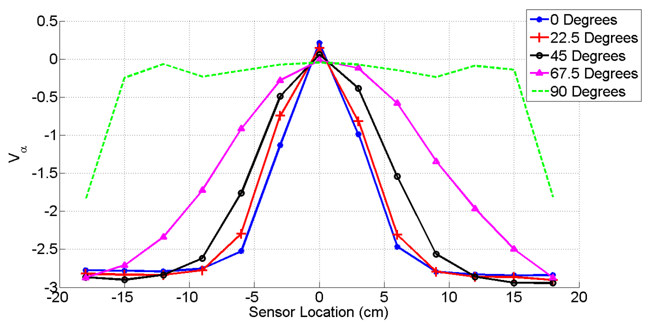

Fig. 6. Observations on locating reinforcement rod at sensor placed 20 mm above the reinforcement rod.

sensor with the rod, prior to estimating thickness of any overlaying concrete. This can be accomplished by rotating the sensor around its centre and observing variations of V_α through the strategy illustrated in Fig. 4. Experiment 2 was conducted to verify this strategy and the experimental set–up used is illustrated in Fig. 7. A sample reinforcement rod was placed 30 mm right beneath the sensor as in Fig. 7, and V_α was recorded for different angles. Variation of V_α observed is plotted in Fig. 8. As per Fig. 8, it can be seen that the maximums of V_α result when the rod is aligned with the long side of the sensor while minimums of V_α result when the rod is at right angles to the sensor. This variation suggests the possibility of aligning the sensor by observing V_α.

C. Experiment 3: Obtaining a function between depth to reinforcement rod and V_α.

Estimating the depth to a reinforcement rod, or in other words, estimating the thickness of concrete or any other non–conductive material overlaying a reinforcement rod becomes the final step required to accomplish wall loss estimation. This can be achieved by calibrating a function between depth to reinforcement rod and V_α. To investigate the existence of a function, V_α was recorded for various depths while the sensor and the rod remained aligned (i.e., 0^0 between the rod and the long side of the sensor). Observed results are available

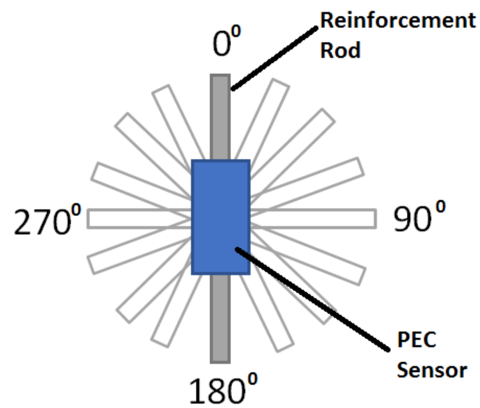

Fig. 7. Experimental set–up for observing influence of sensor alignment on V_α (note that rod orientation relative to the sensor is marked in the figure, the experiment may be conducted either by rotating the sensor or by rotating the rod).

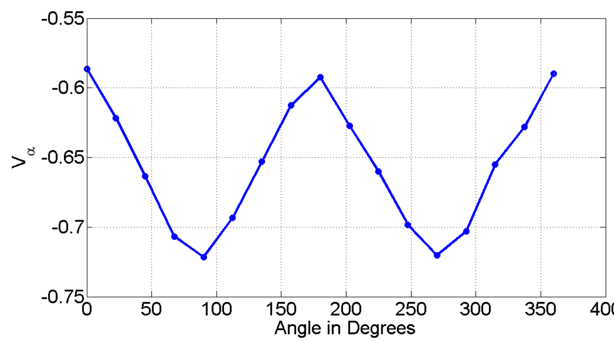

Fig. 8. Observed influence of sensor alignment on V_α at sensor placed 30 mm above the reinforcement rod.

in Fig. 9 and they indeed demonstrate the characteristics of a function, indicating the possibility of estimating unknown depths once calibrated.

In the event of any errors in alignment occurring in practical application, such errors will influence the accuracy of depth estimates. To verify the degree of errors that would occur in depth estimates, V_α was recorded for various depths for the instances where the rod is misaligned by 45^0 and 90^0, where the 90^0 case is considered as the worst case scenario. Observed results are shown in Fig. 10. As evident in Fig. 10, the function–like behaviour remains preserved all the way to the 90^0 worst case scenario, and the resulting errors appear to be acceptable. At low depths of around 5 mm, the errors can be as high as about 5 mm, while at high depths of about 50 mm (the maximum that was expected for the work of this paper), the errors could be as low as 2 or 3 mm, suggesting possibility of estimating depths to reinforcement rods even in the presence of some misalignment.

D. Experiment 4: Influence on V_α by adjacent reinforcement rods.

Since PEC sensors have a domain of influence due to them operating by means of emitting a magnetic field, and the function for concrete thickness estimation (Fig. 9) would typically be calibrated using one reinforcement rod aligned and placed vertically beneath the sensor, it becomes important to characterize any errors that might result due to multiple reinforcement rods being available in the vicinity of the sensor. Quite often inside real sewer walls, parallel reinforcement rods will be available beneath the sensor, usually on a plane that is parallel to the sensor. To study the influence on V_α caused by multiple reinforcement rods placed as such, the experiment illustrated in Fig. 11 was conducted. Three reinforcement rods (rods of 12 mm diameter as in the rest of the experiments) were placed aligned and parallel to the sensor. For a fixed depth to the rods, distance x (in Fig. 11) was varied from 0 to 15 cm in steps of 3 cm. This was repeated for different depths so that the influence on the depth estimation function in Fig. 9 could be studied. Observed results are shown in Fig. 12 and 13. As per the results in Fig. 12, a distance as close as 6 cm between 12 mm rods tend to cause very little influence (i.e., errors of no more than to 2 or 3 mm) on the depth estimation function for the particular PEC sensor used in this work. On the contrary, as shown in Fig. 13, distances as close as 0 and 3 cm appear to cause a significant influence on the depth estimation function. One can conduct such experiments and use observations such as those in Fig. 12 and 13 to provide useful recommendations on the minimum spacing between reinforcement rods that will be bearable for a particular PEC sensor selected for a reinforced concrete assessment task.

V. Conclusions

The paper addressed the problem of condition assessment of reinforced concrete. Strategies to accomplish the task using PEC sensing were presented along with experimental results which verify the strategies. A PEC signal feature (V_α) was proposed and used for the work. Experimental results showed that V_α can be used to locate reinforcement rods, to align the sensor to a rod, and to eventually estimate the depth to a reinforcement rod. Based on those results, it can be concluded that PEC sensors show great potential in reinforced concrete condition assessment through wall loss estimation, which is useful for demanding tasks such as concrete sewer condition assessment, especially since certain PEC sensors come with an established capability to readily interface with robotic platforms. Future work should focus on employing PEC sensors in challenging environments such as concrete sewers to further test and evaluate the condition assessment strategies proposed in this paper.

Acknowledgment

This publication is an outcome from the 'Development of Sensor Suites and Robotic Deployment Strategies for Condition Assessment of Concrete Sewer Walls' project funded by the Sydney Water Corporation.

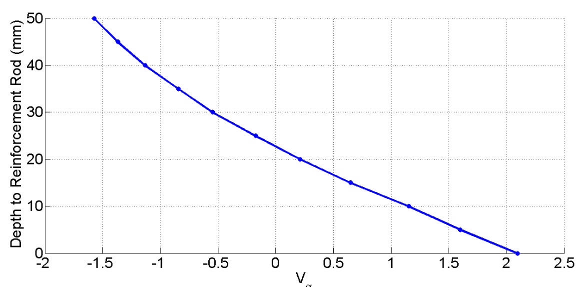

Fig. 9. Function between depth to reinforcement rod and V_α when the rod and the sensor are aligned.

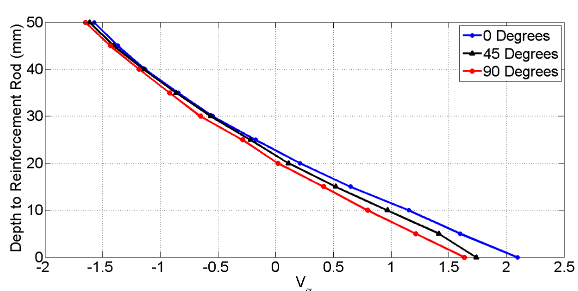

Fig. 10. Functions between depth to reinforcement rod and V_α in the presence of misalignment between the rod and the sensor.

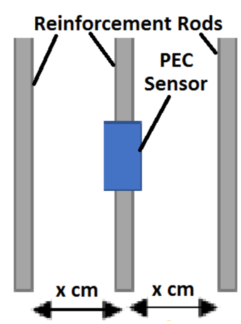

Fig. 11. Experimental setup for observing influence on V_α by adjacent reinforcement rods.

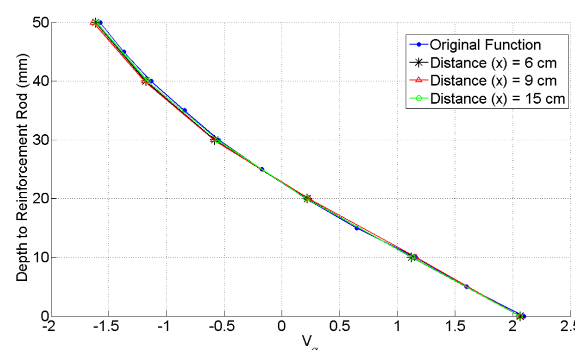

Fig. 12. Influence on the function between depth to reinforcement rod and V_α, in the presence of three adjacent reinforcement rods (x = 6, 9, and 15 cm cases).

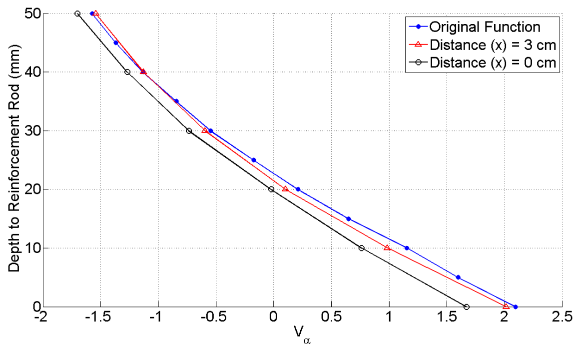

Fig. 13. Influence on the function between depth to reinforcement rod and V_α in the presence of three adjacent reinforcement rods ($x = 0$, and 3 cm cases).

REFERENCES

[1] J. García-Martín, J. Gómez-Gil, and E. Vázquez-Sánchez, "Non-destructive techniques based on eddy current testing," *Sensors*, vol. 11, no. 3, pp. 2525–2565, 2011.

[2] C. Huang, X. Wu, Z. Xu, and Y. Kang, "Ferromagnetic material pulsed eddy current testing signal modeling by equivalent multiple-coil-coupling approach," *NDT & E International*, vol. 44, no. 2, pp. 163–168, 2011.

[3] C. Huang and X. Wu, "An improved ferromagnetic material pulsed eddy current testing signal processing method based on numerical cumulative integration," *NDT & E International*, vol. 69, pp. 35–39, 2015.

[4] L. Nguyen, N. Ulapane, J. Valls Miro, G. Dissanayake, and F. Munoz, "Improved signal interpretation for cast iron thickness assessment based on pulsed eddy current sensing," in *12th IEEE Conference on Industrial Electronics and Applications*, 2017.

[5] N. Ulapane, L. Nguyen, J. Valls Miro, and G. Dissanayake, "A solution to the inverse pulsed eddy current problem enabling 3d profiling," in *IEEE Conference on Industrial Electronics and Applications*, 2018.

[6] Z. Liu and Y. Kleiner, "State of the art review of inspection technologies for condition assessment of water pipes," *Measurement*, vol. 46, no. 1, pp. 1–15, 2013.

[7] J. V. Miro, J. Rajalingam, T. Vidal-Calleja, F. de Bruijn, R. Wood, D. Vitanage, N. Ulapane, B. Wijerathna, and D. Su, "A live test-bed for the advancement of condition assessment and failure prediction research on critical pipes," in *Proceedings of the Leading-Edge Strategic Asset Management Conference (LESAM13)*, 2013.

[8] N. Ulapane, A. Alempijevic, T. Vidal-Calleja, J. V. Miro, J. Rudd, and M. Roubal, "Gaussian process for interpreting pulsed eddy current signals for ferromagnetic pipe profiling," in *Industrial Electronics and Applications (ICIEA), 2014 IEEE 9th Conference on*. IEEE, 2014, pp. 1762–1767.

[9] A. M. N. N. B. Ulapane, "Nondestructive evaluation of ferromagnetic critical water pipes using pulsed eddy current testing," Ph.D. dissertation, 2016.

[10] N. Ulapane, A. Alempijevic, T. Vidal Calleja, and J. Valls Miro, "Pulsed eddy current sensing for critical pipe condition assessment," *Sensors*, vol. 17, no. 10, p. 2208, 2017.

[11] N. Ulapane, A. Alempijevic, J. V. Miro, and T. Vidal-Calleja, "Non-destructive evaluation of ferromagnetic material thickness using pulsed eddy current sensor detector coil voltage decay rate," *NDT & E International*, vol. 100, pp. 108–114, 2018.

[12] K. Thiyagarajan, S. Kodagoda, and J. K. Alvarez, "An instrumentation system for smart monitoring of surface temperature," in *2016 14th International Conference on Control, Automation, Robotics and Vision (ICARCV)*. IEEE, 2016, pp. 1–6.

[13] K. Thiyagarajan, S. Kodagoda, and L. Van Nguyen, "Predictive analytics for detecting sensor failure using autoregressive integrated moving average model," in *2017 12th IEEE Conference on Industrial Electronics and Applications (ICIEA)*. IEEE, 2017, pp. 1926–1931.

[14] K. Thiyagarajan, "Robust sensor technologies combined with smart predictive analytics for hostile sewer infrastructures," Ph.D. dissertation, 2018.

[15] K. Thiyagarajan, S. Kodagoda, L. Van Nguyen, and R. Ranasinghe, "Sensor failure detection and faulty data accommodation approach for instrumented wastewater infrastructures," *IEEE Access*, vol. 6, pp. 56 562 – 56 574, 2018.

[16] K. Thiyagarajan, S. Kodagoda, R. Ranasinghe, D. Vitanage, and G. Iori, "Robust sensing suite for measuring temporal dynamics of surface temperature in sewers," *Scientific Reports*, vol. 8, no. 16020, 2018.

[17] K. Thiyagarajan, S. Kodagoda, L. Nguyen, and S. Wickramanayake, "Gaussian markov random fields for localizing reinforcing bars in concrete infrastructure," in *35th International Symposium on Automation and Robotics in Construction*. IAARC, 2018, pp. 1052–1058.

[18] K. Thiyagarajan, S. Kodagoda, and N. Ulapane, "Data-driven machine learning approach for predicting volumetric moisture content of concrete using resistance sensor measurements," in *2016 IEEE 11th Conference on Industrial Electronics and Applications*. IEEE, 2016, pp. 1288–1293.

[19] D. McCann and M. Forde, "Review of ndt methods in the assessment of concrete and masonry structures," *Ndt & E International*, vol. 34, no. 2, pp. 71–84, 2001.

[20] J. Alldred, "Improvement to the orthogonal method for determining reinforcing bar diameter using a cover meter," in *Conference Proceedings of Structural Faults and Repair*, vol. 2, 1995, pp. 11–15.

[21] J. V. Miro, D. Hunt, N. Ulapane, and M. Behrens, "Towards automatic robotic ndt dense mapping for pipeline integrity inspection," in *Field and Service Robotics*. Springer, 2018, pp. 319–333.

[22] J. Valls Miro, N. Ulapane, L. Shi, D. Hunt, and M. Behrens, "Robotic pipeline wall thickness evaluation for dense nondestructive testing inspection," *Journal of Field Robotics*, vol. 35, no. 8, pp. 1293–1310, 2018.

[23] N. Ulapane, L. Nguyen, J. V. Miro, A. Alempijevic, and G. Dissanayake, "Designing a pulsed eddy current sensing set-up for cast iron thickness assessment," in *Industrial Electronics and Applications (ICIEA), 2017 12th IEEE Conference on*. IEEE, 2017, pp. 901–906.